Asymmetric Intraguild Predation Between *Protoperidinium* and *Heterocapsa* in the Presence of a Mutual Predator

Laura Asaro[1], Joanna Myers[2], Carlos C. Vera Recio[3], Alan Wirkus-Camacho[4], Miles Manning[5],Yiqiang Zheng[6], Baojun Song[7]

[1] Department of Mathematics and Computer Science, East Central University, Ada, OK
[2] Department of Mathematics, University of North Carolina, Asheville, NC
[3] Department of Biology, University of Puerto Rico, Mayagüez, PR
[4] Herberger Young Scholars Academy, Glendale, AZ
[5] School of Human Evolution and Social Change, Arizona State University, Tempe, AZ
[6] Department of Mathematics, Purdue University, West Lafayette, IN
[7] Department of Mathematical Sciences, Montclair State University, Montclair, NJ

Abstract

The azaspiracid toxin contaminated the harvest of the mussel, *Mytilus edulis*, off the coast of Ireland in 1995. Investigation showed that the genus *Protoperidinium*, previously thought to be harmless, was to blame for a new condition brought about by the azaspiracid toxin. To address this concern, we use nonlinear ordinary differential equations to study the dynamics of two dinoflagellate species, as well as their common predator. An asymmetric intraguild predation model with a mutual predator is introduced, in which the toxin producing *Protoperidinium* preys on the non-toxic *Heterocapsa*, while both ingest the nutrients available in the system and are preyed upon by a higher predator. The equilibria were found and global and local stability was determined. We then found the mode of coexistence of the system in an equilibrium. After the initial analysis, we considered interventions, such as modifying nutrient flow, to reduce the levels of the azaspiracid toxin and observe their effect on the persistence of the system.

1 Introduction

Mytulis edulis, more commonly known as the blue mussel, is an economically relevant resource harvested by countries around the world. One noteworthy population can be found in Killary Harbour (located on the West coast of Ireland) where seasonal harvesting of *M. edulis* began in the 1980s. After over a decade of production that did not result in any cases of shellfish poisoning, there was an outbreak of reported illnesses relating to the consumption of the mussels exported from Killary Harbour to other European nations. First reported in November of 1995 in the Netherlands [9], only 8 cases of the illness were recorded [21]. The accompanying symptoms were nausea, vomiting, severe diarrhea, and stomach cramps [9]. Unfortunately it is thought that numerous cases of this poisoning were left unreported or improperly categorized due to the fact that many people deduced that the affliction they were suffering from was either diarrheal shellfish poisoning (DSP) or paralytic shellfish poisoning (PSP), which is caused by organisms belonging to *Alexandrium* spp. as well as *Dinophysis* spp. [9]. Further investigation revealed that this poisoning was

not due to the toxins that lead to DSP or PSP, but rather a new toxin, azaspiracid [21]. Several more confirmed reports of azaspiracid poisoning (AZP) soon followed, affecting twelve additional individuals [9]. In total, dozens of cases were recorded in the years following the initial discovery of AZP. The origin of this toxin was soon found to be generated by members of the genus *Protoperidinium*, a group of dinoflagellate phytoplankton common to numerous areas of the world [9]. Fortunately, no cases of AZP have been known to cause death. However, evidence shows that toxic phytoplankton blooms are increasing worldwide, likely due to climate change and human interaction with the environment [9]. To protect human health and shellfish harvesters, it has become critical to monitor phytoplankton blooms and to seek understanding of the life cycles and relationships that exist between these microorganisms. Due to the discovery of this toxin, regulations have been set in place to protect the consumer population from ingesting this harmful chemical [21].

Since the discovery of this toxic trait of *Protoperidinium*, this particular phytoplankton has been of great interest to biologists, ecologists, chemists, and mathematicians worldwide. In light of this fact, much has been studied and determined about species of *Protoperidinium*. Phytoplankton thrive in nitrogen rich environments and grow by cell division. Though life spans of phytoplankton tend to be very short (ranging from hours to days), they are microorganisms that contribute significantly to the food web as well as the process of moving nutrients from the environment to higher predators [15]. *Protoperidinium* are dinoflagellates that are primarily heterotrophic, requiring sustenance from their environment. [10]. Though they are known to feed predominately on diatoms and bacteria, in some instances such as red tide events, they have been known to prey on other dinoflagellates [9, 10]. Members of *Protoperidinium* consume their prey by means of a pallium [12]. This is a temporary projection from the cell which allows it to digest other phytoplankton that could be of a wide size range.

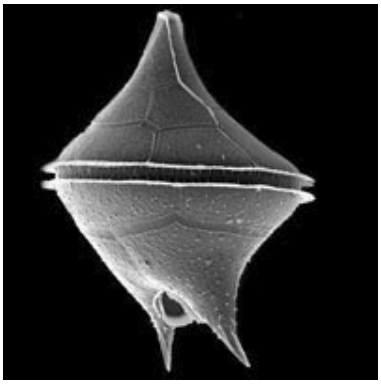

mnh.si.edu

Figure 1: *Protoperidinium crassipes*, a known producer of the azaspiracid toxin.

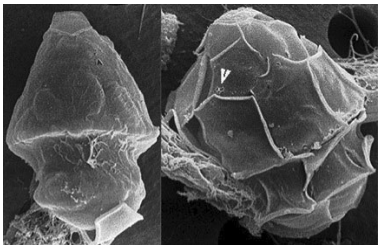

media.nordicmicroalgae.org

Figure 2: An example of a member of the genus *Heterocapsa*.

One genus that *Protoperidinium* preys upon is *Heterocapsa*, a medium sized dinoflagellate. The average size of *Heterocapsa* is 1180 μm^3, whereas its predator, *Protoperidinium*, averages 92,000 μm^3 [17]. The *Heterocapsa* is mixotrophic, which means it has the option of taking in nutrients from the environment or using photosynthesis for energy or a combination of both. Both of these species are distributed around the world and are found mainly in coastal and estuarine waters [16]. In environments containing phytoplankton dinoflagellate species, many types of zooplankton are often found [8]. Zooplankton are generally larger than phytoplankton and prey on these smaller organisms. Unlike their prey, zooplankton are unable to fix their own nitrogen and require the presence of others to feed on. Though *M. edulis* also feeds on the two phytoplankton previously mentioned, it is a filter feeder and is not selective when it chooses its prey. For this reason we choose to focus on the relationship among our two dinoflagellate and a more discerning predator to create an accurate representation of the population dynamics of a

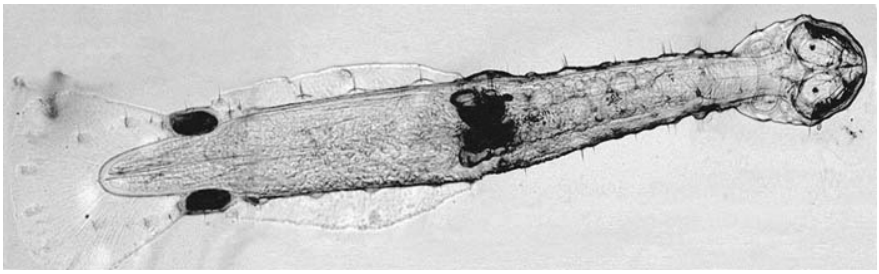

www.microscopy-uk.org.uk/mag/ind

Figure 3: *Chaetognath*, more commonly known as the arrow worm.

selected area of the environment, namely Massachusetts' Bay. For our model, we choose a specific zooplankton, the *Chaetognath*, which reproduces sexually, has an average life span of three to six months, and preys on both of our phytoplankton species [3].

Though the incident caused by this toxin began in Ireland, high volumes of *Protoperidinium* have also been found in US coastal waters in recent years. Studies at Massachusetts Bay were conducted from 1992 to 2007 in which concentrations of *Protoperidinium* were recorded. Due to these findings, it is reasonable to expect that an event such as the one in Killary Harbour can also occur in Massachusetts Bay [8]. The bay is located in an urbanized area of Massachusetts where hundreds of millions of gallons of sewage are pumped daily. Since it is theorized that continuous climate alteration as well as human activity, such as releasing sewage into the ocean, can increase phytoplankton levels [9], it is evident that the analysis of these species within Massachusetts Bay is meaningful.

Conclusive evidence that pollution is the cause of increasing toxic blooms is currently nonexistent. In fact, there are many possible causes, including weather and ocean variability. Nonetheless, there remains the possibility that human behavior may be increasing nutrient levels in coastal waterways [8]. In the year 2000, the Massachusetts Water Resources Authority (MWRA) relocated sewage treatment plant discharge from the Boston Harbor to a site approximately nine miles offshore in the Massachusetts Bay. An extensive study was conducted for several years leading up to the relocation and for several years afterward in order to examine the impact of the relocation and any resulting change upon the zooplankton and phytoplankton populations in the affected areas [8]. As a result of the 16 year MWRA study, we are fortunate to have extensive data concerning the populations of planktons in the area. We incorporate this data in our model's structure in order to study the dynamics between toxin and non-toxin producing phytoplankton. From the analysis, it would certainly be beneficial to find a control mechanism to decrease the ratio of toxin to non-toxin producing phytoplankton. Although there has been no record of azaspiracid poisoning in the Massachusetts Bay area, it has the necessary elements to allow this situation to occur. Therefore, monitoring and investigation is critical.

While it may seem necessary to monitor the growth of only *Protoperidinum*, one must also take into consideration the growth of its prey, *Heterocapsa*. Although *Heterocapsa* is non-toxic, the conditions that have caused a dramatic increase in dense blooms worldwide are the same conditions that have allowed a surge in toxic blooms. Research shows that altered nutrient levels are an important factor lending to such algae proliferation [18]. Since nitrogen is a limiting nutrient for algae [18], we consider that a possible control mechanism to decrease the toxin-producing phytoplankton might be controlling oceanic nitrogen levels.

2 Intraguild Predation

Predator prey, consumer resource, and competition models can be very useful for analyzing interspecies dynamics. Although these models have proven helpful in numerous studies, most relationships between species tend to contain vast complications. Trying to more articulately discuss the interactions of an ecosystem brought about the idea of a new type of model known as intraguild predation (IGP) [7]. Intraguild predation can be seen as one element of a very complex food web [7]. A guild is defined as a collection of species that takes advantage of the same class of environmental resources in a similar way [1]. Since the analysis of food webs of entire ecosystems is impractical (especially within the ocean), these smaller models that focus on one trophic level can reveal information not visible by others. The trophic level of any organism refers to the tier it occupies in the food web. Intraguild predation models focus on competition and predator prey relations within these trophic levels. Not only do they consider two species sharing the same resource, they take into account that one of these species (IGpredator) can gain sustenance by eating the other (intermediate species or IGprey) [7]. Another condition on the IGP model is that the IGpredator be a less successful consumer on the basal resource than the IGprey. Similar to other population models, intraguild predation can vary depending on species interactions. IGP models can highlight changes in population that may not immediately be evident from other models, such as a sudden decrease in an IGprey when a shared top predator outside the guild is eliminated. This is due to the fact that the IGpredator is allowed to increase in abundance and is no longer held in check by the top predator [7].

Studies that employ IGP models are increasing, and many of these combine the standard IGP with other, more well known types of population dynamic models [2, 6, 7, 13]. When applied to a competition Lotka-Volterra predator-prey model [7], complexity is significantly increased as compared to the standard Lotka-Volterra predator-prey model. This increased complexity is common in applications of IGP to models. The reason is easy to see as it adds another layer of interaction between the competing species. It is generally very difficult to isolate coexistance between the IGpredator and IGprey. There are hypotheses that integrating adaptive grazing techniques, such as switching between food resources, could create stable states that are easier to isolate. Specifically, they may create more opportunities for the IGprey to remain present in the model.

2.1 Symmetric Intraguild Predation

In some cases IGP occurs symmetrically, where two competing species both prey on each other as well as their shared resource. This type of model is used frequently to determine the relationship between native and invasive species [13]. When an invasive species is first introduced into an environment, populations of organisms within the food web can be severely disrupted. Regarding the non-native species, predation by a higher predator is usually lower than it is on the native species occupying the same niche. This is due to the unfamiliarity of predators with this new type of prey. When this occurs, the new species gains an advantage and can easily drive the native predator to extinction. Studies and data show that coexistence depends greatly on the amount of basal resource available [2]. Information such as this can aid our understanding of a more complicated system, and lead us to notice in our model that the input of nutrients into the system may have the greatest effect on the entire set of interactions.

2.2 Asymmetric Intraguild Predation

An alternative to symmetric intraguild predation is asymmetric intraguild predation which deviates from symmetric only slightly, but integrates much different dynamics. In this case, only one of the predators can feed on the species that shares its trophic level and basal resource [19]. It is clear that these dynamics may make it difficult to achieve a stable state in which all entities within the system remain present. While more difficult to interpret, this model is a very accurate way to think about the interactions that take place in food webs. Again, in this case it is possible to include a higher predator that is of a different trophic level than the IGpredator and IGprey.

3 Mathematical Models of Asymmetric IGP

3.1 Use of IGP in Our Model

Protoperidinium and *Heterocapsa* compete for the same resources while also engaging in predator-prey interactions; thus they participate in intraguild predation [7]. We also choose to include a higher predator in our model, *Chaetognatha* a genus of zooplankton, to more accurately represent the environment in which these phytoplankton exist. Because of this, we consider our model to be an intraguild predation model (IGP), with the addition of a mutual predator. The motivation to include a higher predator is the ability to keep the IGpredator in check since our model is asymmetric. Furthermore, the fact that only one species preys on the other makes this asymmetric intraguild predation [7]. According to Holt et al. [7], there are important requirements necessary in order to maintain successful coexistence of the two IGP competing species. First, the prey should have an advantage in competing for the shared resources. This is true in our system, since in the presence of normal nitrogen levels, *Heterocapsa* is more efficient at nitrogen intake than *Protoperidinium* [18]. Second, the predator should dramatically increase in population due to its consumption of *Heterocapsa* [11]. Finally, it's common in an IGP system to have selective predation on the superior competitor by the top tier predator [11]. The final condition regarding selective predation on *Heterocapsa* is not necessarily true in our case as *Chaetognatha* feeds by sensing vibrations in the water, therefore it is more likely to eat larger prey, such as *Protoperidinium*. This is discussed further in section 8.

3.2 Model Description

Our general model is a system of four ODEs. This model describes the dynamics of the populations of two intermediate predator species, toxic phytoplankton (T) and non-toxic phytoplankton (N), as well as a shared resource, environmental nutrients (E). The model also includes zooplankton as a top predator (Z), which preys on both N and T. As discussed above, we use an asymmetric intraguild predation model (with the addition of a mutual predator) with T preying on N. This model represents the intricate relationship of the three organisms and their basal resource. We also include a constant inflow of nutrients and zooplankton, as well as an outflow.

We now present the general form of our model.

$$E' = G_E(E) - D_E(E) - C_N(E,N) - C_T(E,T) \quad (1)$$
$$N' = c_2 C_N(E,N) - P_{TN}(T,N) - P_{ZN}(Z,N) - D_N(N) \quad (2)$$
$$T' = c_1 C_T(E,T) + m_1 P_{TN}(T,N) - P_{ZT}(Z,T) - D_T(T) \quad (3)$$
$$Z' = G_Z(Z) - D_Z(Z) + m_3 P_{ZN}(Z,N) + m_2 P_{ZT}(Z,T) \quad (4)$$

The system contains four equations that represent the change in nutrients (E'), non-toxic phytoplankton (N'), toxic phytoplankton (T'), and zooplankton (Z') over time. For our specific case we consider a Holling Type 1 functional response for predation rate, which means the predator consumption increases linearly and the predators do not get satiated. We choose to represent a population's size by their biomass. Therefore we need to include conversion factors to account for biomass gained by consumption. Also, for our specific case we choose nitrogen as our nutrient. We now take the general equation and include our parameters. A diagram of this system is shown in Figure 4. By doing this, we generate a system of differential equations that we can use to examine our asymmetric IGP in the presence of a mutual predator.

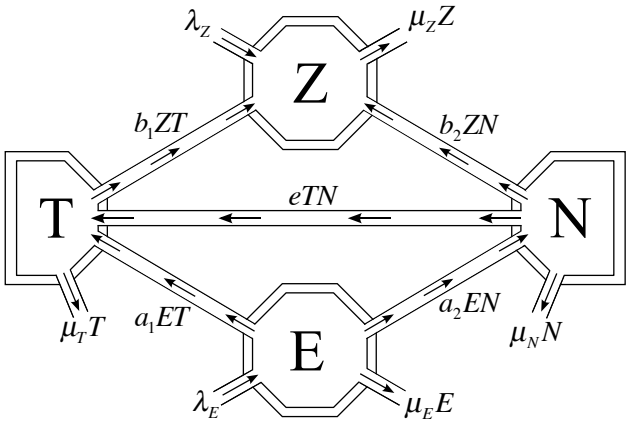

Figure 4: A representational diagram of the flow of energy from the basal resource to the top predator. E, N, T, Z represent nutrients, non-toxic phytoplankton, toxic phytoplankton and zooplankton, respectively.

$$E' = \lambda_E - a_1 ET - a_2 EN - \mu_E E \quad (5)$$
$$N' = a_2 c_2 EN - b_2 ZN - eTN - \mu_N N \quad (6)$$
$$T' = a_1 c_1 ET + m_1 eTN - b_1 ZT - \mu_T T \quad (7)$$
$$Z' = \lambda_Z + b_1 m_2 TZ + b_2 m_3 NZ - \mu_Z Z \quad (8)$$

The parameter λ_i represents the inflow of nitrogen or *Chaetognatha*. With μ_i, we represent the outflow or natural death rate of the respective biomass. Parameter a_i represents the consumption rate of nitrogen by either of the phytoplankton species, while b_i is the predation rate of *Chaetognatha* on a particular photoplankton species. We use parameter e to express the predation rate from *Protoperidinium* to *Heterocapsa*. Finally, both c_i and m_i are conversion factors which express how one biomass is converted to another during a consumption or predation event.

Table 1: Parameter values used in our model with their descriptions.

Parameter	Description
λ_E/μ_E	(inflow of E)(outflow of E)$^{-1}$
λ_Z	inflow of Z
a_1	consumption by T on E
a_2	consumption by N on E
b_1	predation of Z on T
b_2	predation of Z on N
e	predation of T on N
c_1	mass conversion of E to T
c_2	mass conversion of E to N
m_1	mass conversion of N to T
m_2	mass conversion of T to Z
m_3	mass conversion of N to Z
μ_N	outflow of N
μ_T	outflow of T
μ_Z	outflow of Z

4 Analysis

To understand our system of equations we begin by identifying the various equilibria of the system and determining their stability. We identify four types of equilibria when there are no phytoplankton, when toxic phytoplankton is present and non-toxic is not, when non-toxic is present and toxic is not, or when they are in coexistence.

4.1 Phytoplankton Free Equilibrium (PFE)

The PFE is

$$\left(E^* = \frac{\lambda_E}{\mu_E}, N^* = 0, T^* = 0, Z^* = \frac{\lambda_Z}{\mu_Z}\right)$$

To determine the stability of the PFE, we calculate the Jacobian and evaluate it at the equilibrium point. Two of the eigenvalues are always negative ($-\mu_Z$ and $-\mu_E$). The other two are negative when the following two inequalities hold:

$$a_2c_2E^* < \mu_N + b_2Z^*\text{: births of } N \text{ are less than deaths of } N \tag{9}$$

$$a_1c_1E^* < \mu_T + b_1Z^*\text{: births of } T \text{ are less than deaths of } T \tag{10}$$

The first inequality tells that the growth rate of non-toxic phytoplankton is smaller than its outflow (μ_N) combined with the predation of zooplankton. Similarly, the second inequality requires the growth rate of toxic plankton to be lower than its natural death rate combined with the predation of zooplankton. Furthermore, we can prove the global stability of the PFE.

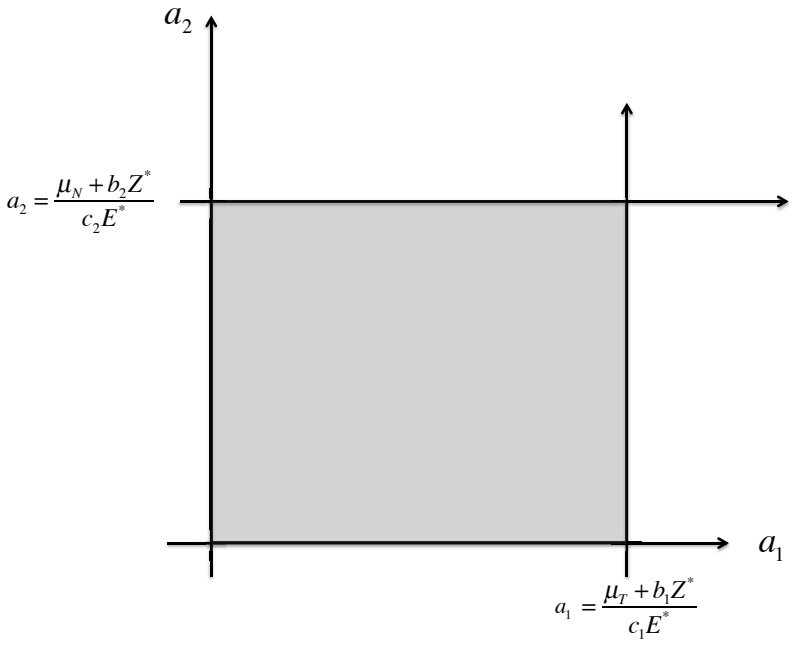

Figure 5: A visual representation of the stability conditions associated with the PFE. In parameter space, the shaded region represents the conditions under which the PFE is stable.

Theorem 1. *If the births of N are less than their deaths and the births of T are less than their deaths at the PFE, then the PFE is globally asymptotically stable.*

Proof. We first show $E \leq E^*$. From equation (5) with N, $T = 0$, we get

$$E' \leq \lambda_E - \mu_E E.$$

Rearranging and multiplying by the integral factor gives

$$e^{t\mu_E} E' + \mu_E e^{t\mu_E} E \leq \lambda_E e^{t\mu_E},$$

which is equivalent to

$$\int_0^t (Ee^{t\mu_E})' dt \leq \int_0^t \lambda_E e^{t\mu_E} dt.$$

Now, taking the integral from 0 to t gives

$$\begin{aligned} Ee^{t\mu_E} - E_0 &\leq \frac{\lambda_E}{\mu_E}(e^{t\mu_E} - 1) \\ Ee^{t\mu_E} &\leq \left(E_0 - \frac{\lambda_E}{\mu_E}\right) + \frac{\lambda_E}{\mu_E} e^{t\mu_E}. \end{aligned}$$

Taking the limit as $t \to \infty$:

$$\lim_{t\to\infty} E \leq \frac{\lambda_E}{\mu_E} + \lim_{t\to\infty} \left(E_0 - \frac{\lambda_E}{\mu_E}\right) e^{-\mu_E t},$$

which is $E \leq E^*$.
By the same process we can show $Z \geq \frac{\lambda_Z}{\mu_Z}$. Now we prove that $N \to 0$ as $t \to \infty$. From equation (6), we obtain

$$\begin{aligned} N' &\leq N(a_2c_2E^* - Z^*b_2 - \mu_N), \\ N' &\leq -\beta N, \end{aligned}$$

where $\beta = -a_2c_2E^* + Z^*b_2 + \mu_N \geq 0$ from equation (9). Again, multiplying by the integral factor gives

$$\begin{aligned} N'e^{\beta t} + \beta N e^{\beta t} &\leq 0 \\ \int_0^t \left(Ne^{\beta t}\right)' dt &\leq \int_0^t 0 \; dt. \end{aligned}$$

Integrating from 0 to t, we have

$$\begin{aligned} Ne^{\beta t} - N_0 &\leq 0 \\ N &\leq N_0 e^{-\beta t}. \end{aligned}$$

Taking the limit as $t \to \infty$

$$0 \leq N \leq \lim_{t\to\infty} N_0 e^{-\beta t}$$

It follows from the Squeeze Theorem that, $N \to 0$ as $t \to \infty$. Now we show that $T \to 0$ as $t \to \infty$. From equation (7), we obtain

$$\begin{aligned} T' &\leq T(a_1c_1E^* - Z^*b_1 - \mu_T), \\ T' &\leq -\gamma T, \end{aligned}$$

where $\gamma = -a_1c_1E^* + Z^*b_1 + \mu_T \geq 0$ from equation (10). Again multiplying by the integral factor, we get

$$\begin{aligned} T'e^{\gamma t} + \gamma T e^{\gamma t} &\leq 0, \\ \int_0^t \left(Te^{\gamma t}\right)' dt &\leq \int_0^t 0 \; dt, \end{aligned}$$

Integrating from 0 to t gives

$$\begin{aligned} Te^{\gamma t} - T_0 &\leq 0 \\ T &\leq T_0 e^{-\gamma t}. \end{aligned}$$

Taking the limit as $t \to \infty$

$$0 \leq T \leq \lim_{t\to\infty} T_{t_0} e^{-\gamma t}$$

It again follows from the Squeeze Theorem that, $T \to 0$ as $t \to \infty$.

Next we show $E \to E^*$ as $t \to \infty$. $E' = \lambda_E - \mu_E E - F(t)E$, where $F(t) = a_1 T + a_2 N$. Since $N \to 0$ and $T \to 0$, $F(t) \to 0$. The limiting equation of E is

$$E' = \lambda_E - \mu_E E.$$

So, we can show $E \to E^*$ as $t \to \infty$.
The process to show $Z \to Z^*$ as $t \to \infty$ is the same as to show $E \to E^*$ as $t \to \infty$. Therefore the PFE $(E^*, 0, 0, Z^*)$ is globally asymptotically stable. ■

4.2 Toxic Phytoplankton Free Equilibrium (TPFE)

Now we analyze the boundary equilibria obtained when the toxic species of phytoplankton is zero, and the non-toxic is non-zero. The TPFE is given by

$$\lambda_E - a_2 EN - \mu_E E = E' = 0 \tag{11}$$
$$a_2 c_2 E - b_2 Z - \mu_N = N' = 0 \tag{12}$$
$$T = T' = 0 \tag{13}$$
$$\lambda_Z + b_2 m_3 NZ - \mu_Z Z = Z' = 0 \tag{14}$$

We first solve equations (11) and (14) for E and Z, respectively to get

$$E_2^* = \frac{\lambda_E}{a_2 N + \mu_E}, \tag{15}$$
$$Z_2^* = \frac{\lambda_Z}{\mu_Z - b_2 m_3 N}. \tag{16}$$

Next we substitute equations (15) and (16) into equation (12). We then obtain the quadratic equation

$$AN^2 + BN + C = 0. \tag{17}$$

where

$$\begin{aligned} A &= \mu_N a_2 b_2 m_3 > 0, \\ B &= b_2 m_3 \mu_E \mu_N - a_2 c_2 \lambda_E b_2 m_3 - \mu_N a_2 \mu_Z - a_2 \lambda_Z b_2, \\ C &= -\mu_E \mu_N \mu_Z + a_2 c_2 \lambda_E \mu_Z - \mu_E \lambda_Z b_1 = \mu_E \mu_Z (-\mu_N + a_2 c_2 \frac{\lambda_E}{\mu_E} - b_1 \frac{\lambda_Z}{\mu_Z}). \end{aligned}$$

Using these substitutions and the quadratic formula we get

$$N_2^* = \frac{-B \pm \sqrt{B^2 - 4AC}}{2A}. \tag{18}$$

Examining the definitions of A, B, and C, we see that $A > 0$ is always true. To have a single positive toxic free boundary equilibrium we need $C < 0$, this is equivalent to

$$\frac{\lambda_E}{\mu_E} a_2 c_2 < \mu_N + \frac{\lambda_Z}{\mu_Z} b_1,$$

which, in conjunction with $T = 0$ implies that the PFE is globally stable. Thus we consider $C > 0$ for the remainder of this discussion.
The Jacobian matrix of the system of equations (1-4) is

$$\begin{bmatrix} -N_2^* a_2 - T_2^* a_1 - \mu_E & -a_2 E_2^* & -a_1 E_2^* & 0 \\ N_2^* a_2 c_2 & 0 & -N_2^* e & -N_2^* b_2 \\ T_2^* a_1 c_1 & m_1 e T_2^* & a_1 E_2^* c_1 + N_2^* e m_1 - Z_2^* b_1 - \mu_T & -T_2^* b_1 \\ 0 & Z_2^* b_2 m_3 & Z_2^* b_1 m_2 & N_2^* b_2 m_3 + b_1 m_2, T_2^* - \mu_Z \end{bmatrix}$$

Substituting $T = 0$, we get the following Jacobian

$$\begin{bmatrix} -N_2^* a_2 - \mu_E & -a_2 E_2^* & -a_1 E_2^* & 0 \\ N_2^* a_2 c_2 & 0 & -N_2^* e & -N_2^* b_2 \\ 0 & 0 & a_1 E_2^* c_1 + N_2^* e m_1 - Z_2^* b_1 - \mu_T & 0 \\ 0 & Z_2^* b_2 m_3 & Z_2^* b_1 m_2 & N_2^* b_2 m_3 - \mu_Z \end{bmatrix}$$

We can see that there is only one nonzero element in the third row, so this is an eigenvalue:

$$\lambda_1 = a_1 E_2^* c_1 + N_2^* e m_1 - Z_2^* b_1 - \mu_T.$$

A condition for stability requires $\lambda_1 < 0$, so

$$a_1 c_1 E_2^* + e m_1 N_2^* - b_1 Z_2^* - \mu_T < 0. \tag{19}$$

Rearranging equation (19), we obtain

$$\begin{aligned} a_1 c_1 E_2^* + e m_1 N_2^* &< b_1 Z_2^* + \mu_T, \\ \text{births of } T &< \text{deaths of } T. \end{aligned}$$

In biological terms, this means that the birth rate due to consumption of nutrients and non-toxic phytoplankton is smaller than the death rate due to predation by zooplankton and outflow. We now reduce the matrix to a 3×3 system.

$$\begin{bmatrix} -N_2^* a_2 - \mu_E & -a_2 E_2^* & 0 \\ N_2^* a_2 c_2 & 0 & -N_2^* b_2 \\ 0 & Z_2^* b_2 m_3 & N_2^* b_2 m_3 - \mu_Z \end{bmatrix}$$

We now obtain our remaining three eigenvalues from J_{TPFE}. We proceed to use Routh-Hurwitz criteria. Calculating the first Routh-Hurwitz parameter, which states that $W_1 = |J_{TPFE}|$must be greater than zero to have stability, we obtain

$$W_1 = (a_2 N_2^* + \mu_E)(b_2 N_2^*)(b_2 m_3 Z_2^*) + a_2 E_2^* (a_2 c_2 N_2^*)(\mu_Z - b_2 m_3 N_2^*)$$

Therefore, $\mu_Z - b_2 m_3 N_2^* > 0$ implies $W_1 > 0$.

Moving on to the second Routh-Hurwitz criteria parameter W_2 = -Tr(J_{TPFE}), we obtain

$$W_2 = a_2N_2^* + \mu_E + (\mu_Z - b_2m_3N_2^*)$$

which must also be greater than zero for stability of the equilibrium point. If we assume the same condition for stability as with W_1, when $\mu_Z - b_2m_3N_2^* > 0$, then $W_2 > 0$. Thus we comply with the requirements for this part of Routh-Hurwitz criteria.

For W_3, the third parameter of Routh-Hurwitz criteria, we get

$$W_3 = (a_2E_2^*)(a_2c_2N_2^*) + (b_2N_2^*)(b_2m_3Z_2^*) + (a_2N_2^* + \mu_E)(\mu_Z - b_2m_3N_2^*) > 0$$

Therefore, if we assume the same condition for stability as with W_1, where $\mu_Z - b_2m_3N_2^* > 0$, then $W_3 > 0$, and we comply with the requirements for this part of Routh-Hurwitz criteria.

The fourth part of Routh-Hurwitz Criteria dictates that $W_2W_3 > W_1$.

$$W_2W_3 = (a_2N_2^*+\mu_E)(b_2m_3Z_2^*)(b_2N_2^*)+(\mu_Z-b_2m_3N_2^*)(a_2E_2^*)(a_2c_2N_2^*)+(a_2N_2^*+\mu_E)[(a_2E_2^*)(a_2c_2N_2^*)+$$

$$(a_2N_2^* + \mu_E)(\mu_Z - b_2m_3N_2^*)] + (\mu_Z - b_2m_3N_2^*)[(b_2N_2^*)(b_2m_3Z_2^*) + (a_2N_2^* + \mu_E)(\mu_Z - b_2m_3N_2^*)$$

We can see that if $\mu_Z - b_2m_3N_2^* > 0$, then $W_2W_3 = W_1 + X$, where $X > 0$. This implies that $W_2W_3 > W_1$. Therefore, we can conclude that if the conditions $\lambda_1 < 0$ and $\mu_Z - b_2m_3N_2^* > 0$ are met, we will have a stable (TPFE) boundary equilibrium.

4.3 Non-Toxic Phytoplankton Free Equilibrium (NTPFE)

For the non-toxic phytoplankton population becoming extinct ($N = 0$), we have:

$$\lambda_E - a_1ET - \mu_EE = E' = 0 \tag{20}$$
$$N = N' = 0 \tag{21}$$
$$a_1c_1E - b_1Z - \mu_T = T' = 0 \tag{22}$$
$$\lambda_Z + b_1m_2TZ - \mu_ZZ = Z' = 0 \tag{23}$$

We solve for E and Z using equations (20) and (23) to achieve

$$E_3^* = \frac{\lambda_E}{a_1T + \mu_E} \tag{24}$$
$$Z_3^* = \frac{\lambda_Z}{\mu_Z - b_1m_2T} \tag{25}$$

Substituting the values for E and Z into equation (22), we obtain the quadratic equation

$$A_TT^2 + B_TT + C_T = 0$$

where

$$A_T = a_1b_1m_2\mu_T$$
$$B_T = b_1m_2\mu_E\mu_T - a_1b_1c_1m_2\lambda_E - a_1b_1\lambda_Z - a_1\mu_T\mu_Z$$
$$C_T = a_1c_1\mu_Z\lambda_E - b_1\mu_E\lambda_Z - \mu_E\mu_T\mu_Z = \mu_E\mu_Z(a_1c_1\frac{\lambda_E}{\mu_E} - b_1\frac{\lambda_Z}{\mu_Z} - \mu_T)$$

With these substitutions we get:

$$T_3^* = \frac{-B_T \pm \sqrt{{B_T}^2 - 4A_T C_T}}{2A_T}$$

Similar to the $T = 0$ boundary equilibria, if $C_T < 0$, then the discriminate is also greater than zero. We would have two real solutions, one positive and one negative. Since $C_T < 0$ implies:

$$\begin{array}{rcl} \frac{\lambda_E}{\mu_E} a_1 c_1 & < & \mu_T + \frac{\lambda_Z}{\mu_Z} b_1 \\ \text{births of } T & < & \text{deaths of } T. \end{array}$$

Which guarantees that the PFE is globally stable since $N = 0$. We consider $C_T > 0$ for the remainder. Now, substituting T into equations (24) and (25)

$$E_3^* = \frac{\lambda_E}{a_1 \frac{-B \pm \sqrt{B^2 - 4AC}}{2A} + \mu_E}$$

$$Z_3^* = \frac{\lambda_Z}{\mu_Z - b_1 m_2 \left(\frac{-B \pm \sqrt{B^2 - 4AC}}{2A} \right)}$$

Theorem 2. *Assume NTPFE exists. If $\mu_Z - b_1 m_2 T_3^* > 0$ and $\lambda_1 < 0$ then the NTPFE is locally asymptotically stable.*

See Appendix B for the accompanying proof.

4.4 Phytoplankton Coexistence Equilibria (PCE)

For the coexistence equilibria where all populations are greater than zero, we have to solve the following equations:

$$\lambda_E - (a_1 T + a_2 N + \mu_E) E = E' = 0 \tag{26}$$
$$a_2 c_2 E - b_2 Z - eT - \mu_N = N' = 0 \tag{27}$$
$$a_1 c_1 E + m_1 eN - b_1 Z - \mu_T = T' = 0 \tag{28}$$
$$\lambda_Z + (b_1 m_2 T + b_2 m_3 N - \mu_Z) Z = Z' = 0 \tag{29}$$

Explicitly, E is given by

$$\lambda_Z + (\tfrac{-A_3}{E} + A_1 E + A_2)[b_1 m_2 (AE - B(\tfrac{-A_3}{E} + A_1 E + A_2) - C) + b_2 m_3 (-DE + F(\tfrac{-A_3}{E} + A_1 E + A_2) + G) - \mu_Z] = 0 \tag{30}$$

and N, T, Z are as follows

$$N_4^* = G - DE + FZ \tag{31}$$
$$T_4^* = AE - BZ - C \tag{32}$$
$$Z_4^* = \frac{-A_3}{E} + A_1 E + A_2, \tag{33}$$

Where

$$A = \frac{a_2 c_2}{e} \qquad D = \frac{a_1 c_1}{m_1 e}$$
$$B = \frac{b_2}{e} \qquad F = \frac{b_1}{m_1 e}$$
$$C = \frac{\mu_N}{e} \qquad G = \frac{\mu_T}{m_1 e}$$

and

$$A_1 = \frac{a_1 A - a_2 D}{a_1 B - a_2 F}$$
$$A_2 = \frac{\mu_E + a_2 G - a_1 C}{a_1 B - a_2 F}$$
$$A_3 = \frac{\lambda_E}{a_1 B - a_2 F}$$

We consider two special cases that reduce this to a cubic equation in the Appendix. We found a single stable coexistence equilibrium for our biologically informed parameters. Work is continued numerically as further analytical attempts prove impracticle.

5 Simulation

We used simulation to explore different values for the parameters λ_E, μ_E, a_1, a_2, and e and to observe the effects on the solution. For our case, we are most interested in the different results gained when varying λ_E and μ_E, as these are parameters we have the ability to control. We begin by showing time series results for non-extinction cases.

Table 2: Parameter values used for simulation.

Parameters	λ_E/μ_E	λ_Z	μ_Z	a_1	a_2	b_1	b_2	e	c_1	c_2	m_1	m_2	m_3	μ_N	μ_T
Value	1.3924	0.75	0.7	1	1.3	0.34	0.1	0.5	60	78.125	0.3	0.1	0.1	1	0.9
Resource	[4]	est.	est.	est.	[23]	est.	est.	[5] [22]	[22]	[22]	[20]	[20]	est.	est.	est.

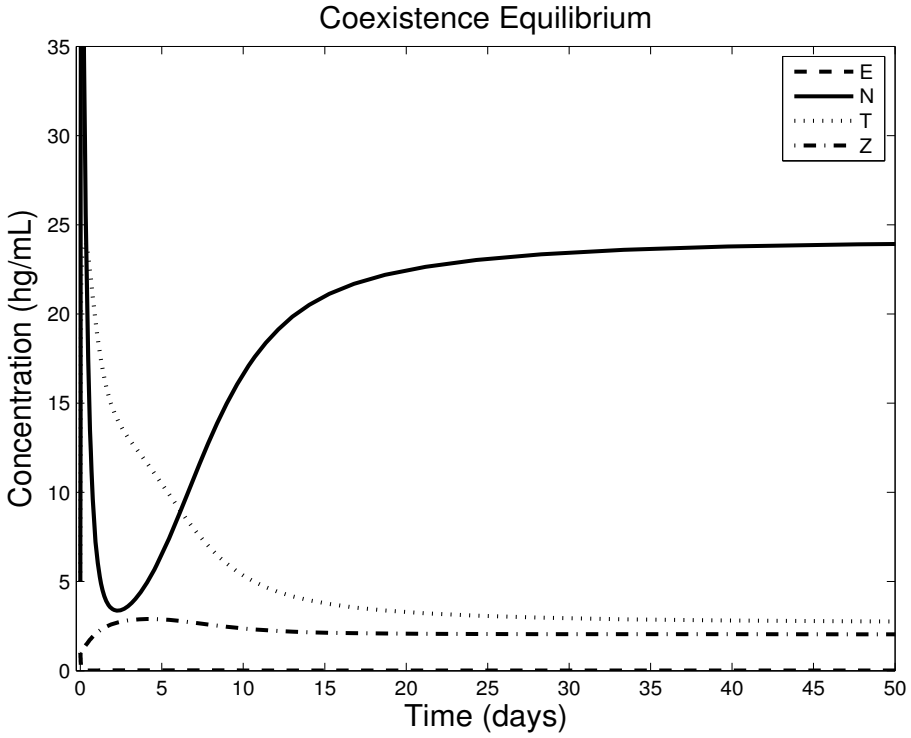

Figure 6: Time series of our model converging to an equilibrium in which every population is non-zero. To generate the figure we consider the parameters in Table 2, the initial conditions $E_0 = 1$, $N_0 = 5$, $T_0 = 5$, and $Z_0 = 1$ as well as $\lambda_E = 0.5$, $\mu_E = 0.3591$ and $e = 0.1$.

In Figure 6 we see that both phytoplankton populations quickly jump to levels that are much higher than their initial conditions. This is because the initial nitrogen concentration is relatively high leading to explosive growth. After the exhaustion of resources the phytoplankton population begins to fall. Toxic phytoplankton fall more slowly than non-toxic because the toxic phytoplankton are able to feed on their non-toxic counterpart. As phytoplankton populations decline, zooplankton grow to carrying capacity. Toxic phytoplankton die off down to their equilibrium state, and once they are sufficiently low, the non-toxic phytoplankton are able to grow up to capacity.

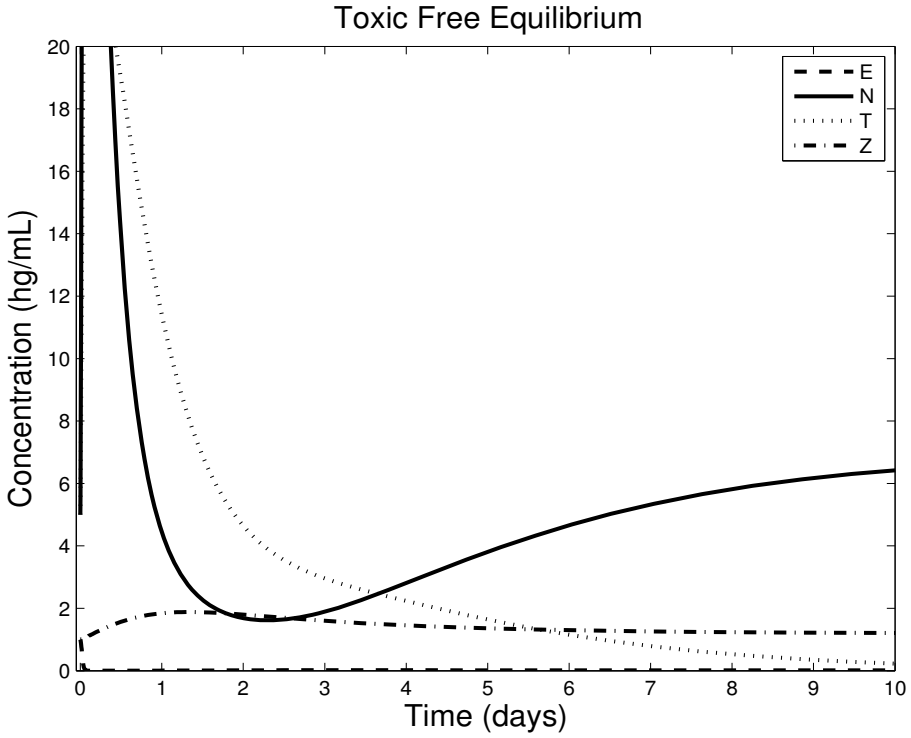

Figure 7: Time series of our model converging to an equilibrium in which the toxic population goes to zero. To generate the figure we consider the parameters in Table 2, the initial conditions $E_0 = 1$, $N_0 = 5$, $T_0 = 5$, and $Z_0 = 1$ as well as $\lambda_E = 0.1$, $\mu_E = 0.07182$ and $e = 0.1$.

In Figure 7, we decrease the flow of nitrogen, which decreases the maximum density of plankton. This also increases the competition over nitrogen. Since non-toxic phytoplankton outcompete toxic phytoplankton in nitrogen intake, toxic phytoplankton are driven to extinction. Note that even though non-toxic phytoplankton are the only phytoplankton in this case, the final density is less than that of the coexistence case. This is simply due to the decreased amount of resources in the environment.

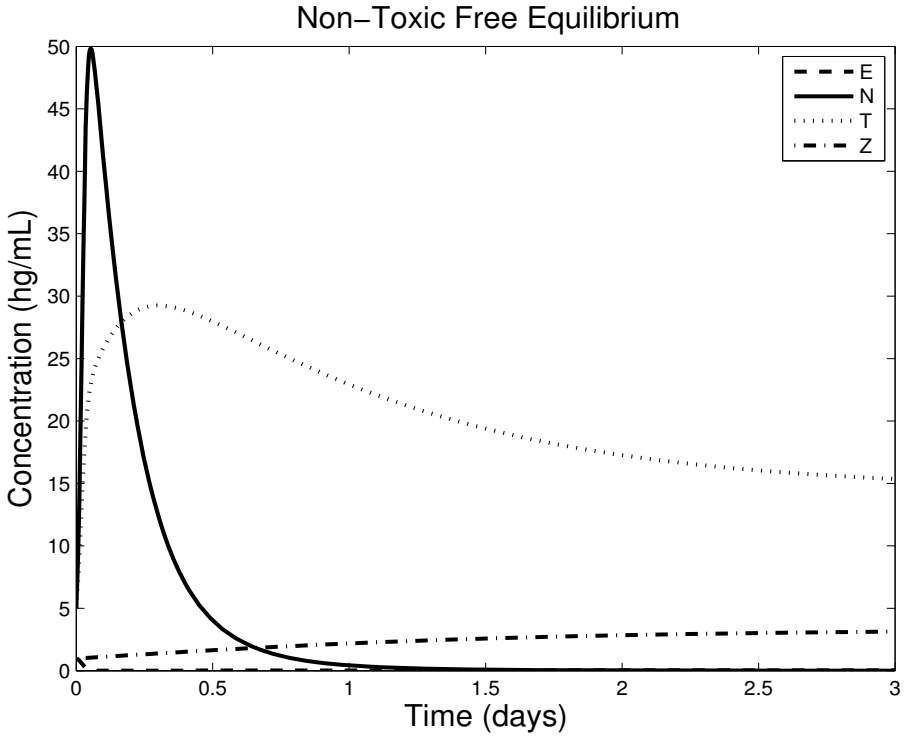

Figure 8: Time series of our model converging to an equilibrium in which the non-toxic population goes to zero. To generate the figure we consider the parameters in Table 2, the initial conditions $E_0 = 1$, $N_0 = 5$, $T_0 = 5$, and $Z_0 = 1$ as well as $\lambda_E = 0.5$, $\mu_E = 0.3591$ and $e = 0.2$.

The beginning of Figure 8 is similar to that of Figure 6. However, the increased predation by toxic phytoplankton on non-toxic phytoplankton causes the extinction of non-toxic phytoplankton following the scarcity of nitrogen. Because of the lack of non-toxic phytoplankton the carrying capacity of toxic phytoplankton is higher than in the coexistence case.

Table 3: Bistable Phase Portrait Parameters

Parameters	λ_E/μ_E	λ_Z	μ_Z	a_1	a_2	b_1	b_2	e	c_1	c_2	m_1	m_2	m_3	μ_N	μ_T
Estimate	1.3924	0.75	0.7	1	1.3	0.7	0.4	0.5	60	78	0.3	0.1	0.1	1	0.9
Resource	[4]	est.	est.	est.	[23]	est.	est.	[5] [22]	[22]	est.	[20]	[20]	est.	est.	est.

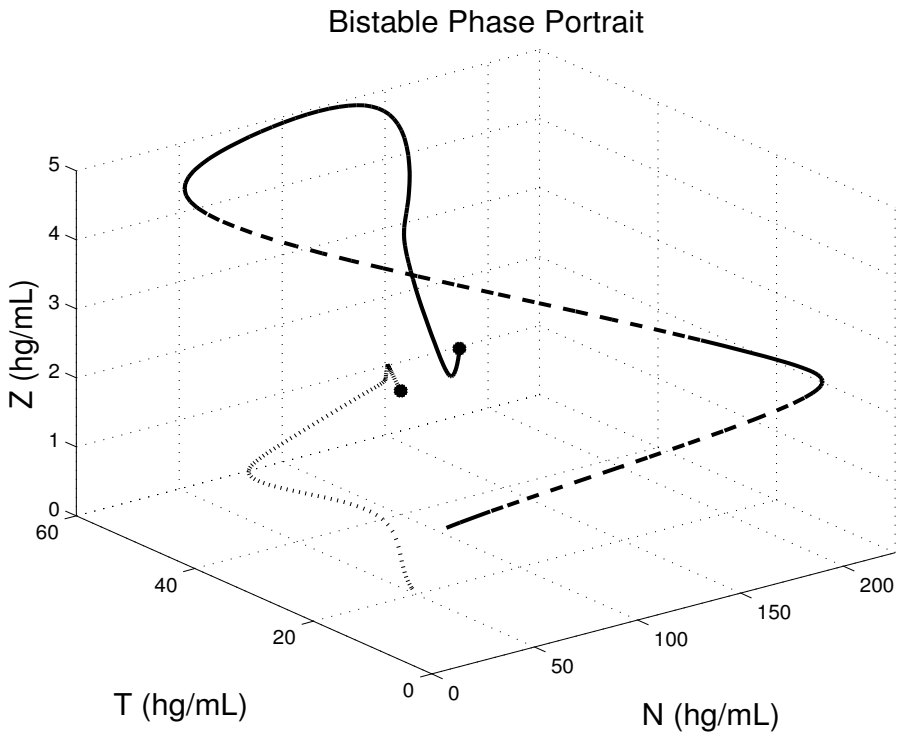

Figure 9: Phase Portrait for Coexistence: This figure was generated using the parameters in Table 3.

Figure (9) is the phase portrait of our model for a parameter set that is bistable. The two stable equilibria are coexistence and toxic free conditions. Interestingly, the coexistence case has a high portion of toxic phytoplankton. From these figures we can see that the equilibria the solution converges to depends primarily on the density of zooplankton when toxic phytoplankton are near extinction.

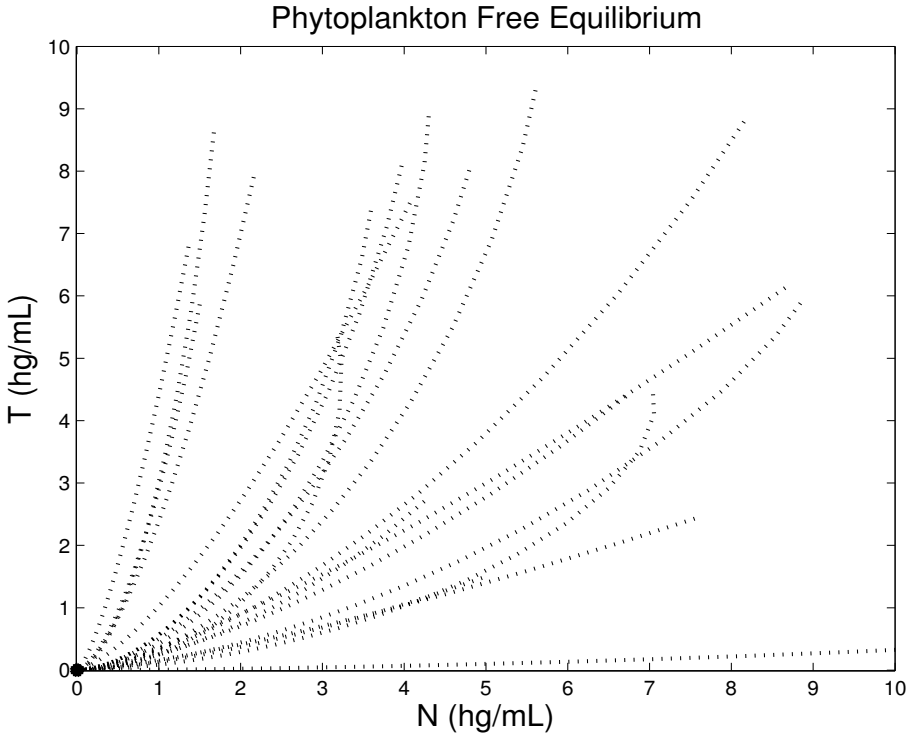

Figure 10: Phase portrait for phytoplankton free equilibrium: non-toxic vs. toxic. This figure was generated using random initial conditions and parameters that fit the stability conditions of the PFE.

Our final simulation shown in Figure 10 demonstrates the global stability of the phytoplankton free equilibrium. To obtain this figure we had to assume incredibly high levels of predation. This demonstrates robustness in the phytoplankton population. Algal blooms take place in ways very similar to the simulations we have conducted. They tend to grow very quickly and do not last long before achieving a steady state in which side effects are not experienced.

6 Ratio of *Protoperidinium* to Total Phytoplankton

Since mussels are filter feeders, they do not discern their prey. By reducing the fraction of total phytoplankton that are toxic, we will be reducing the amount of toxin that mussels consume. Figures 11 through 13 demonstrate the effect on this ratio of nitrogen flow, nitrogen uptake by toxic phytoplankton, intraguild predation, and the presence of a mutual predator. Figure 11 is critical to our work as it shows a range in which nitrogen concentration is at a level that supports a low toxic to non-toxic ratio. Notice that we reach a peak when λ_E is approximately 0.7, and then declines above and below. This is likely due to the fluctuation of non-toxic phytoplankton in total which affects the food source for the toxic phytoplankton. This shows that control of the ratio of harmful phytoplankton can be carried out through the monitoring of nitrogen deposit (λ_E).

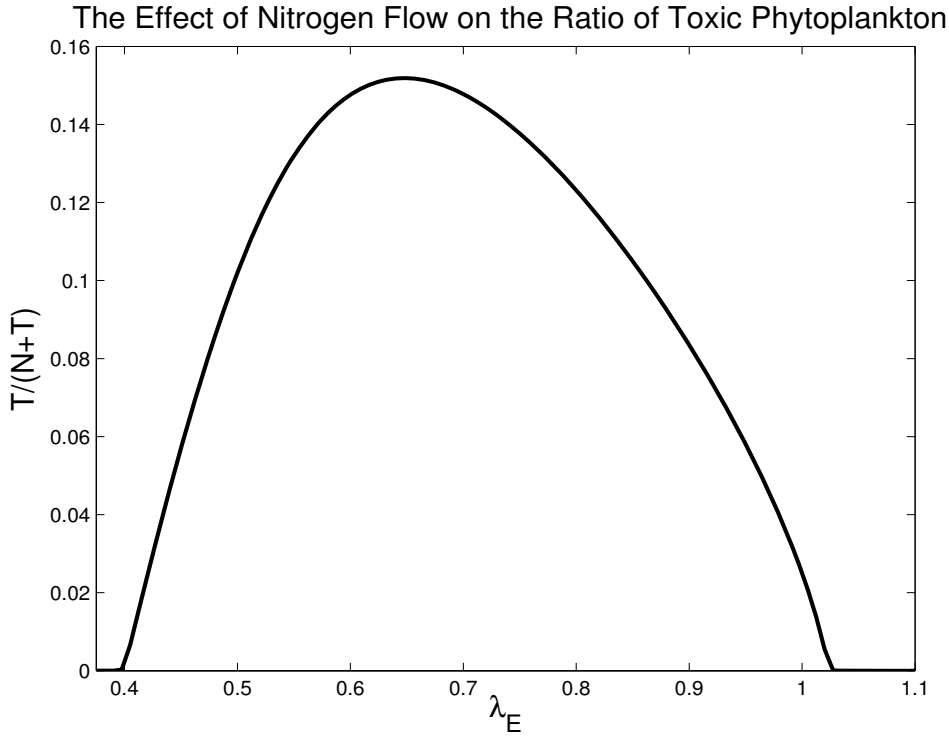

Figure 11: The relationship between nitrogen flow (μ_E varies with λ_E) and the toxic to non-toxic ratio.

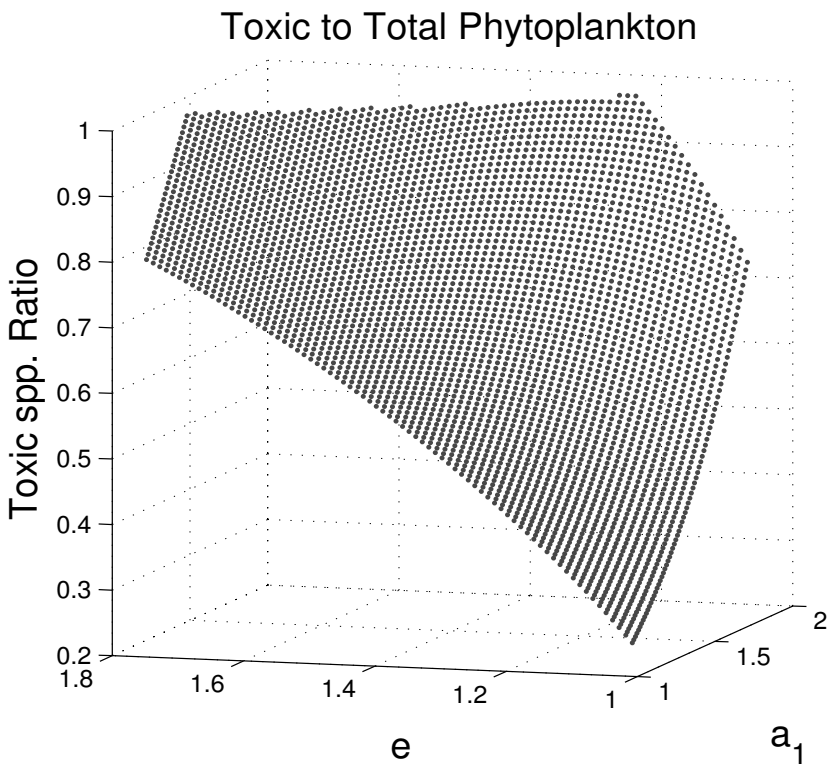

Figure 12: Comparison of the effect of toxic spp. nitrogen uptake rate (a_1) vs. their predation on the non-toxic spp. (e) and their effects on the ratio $\frac{T}{N+T}$.

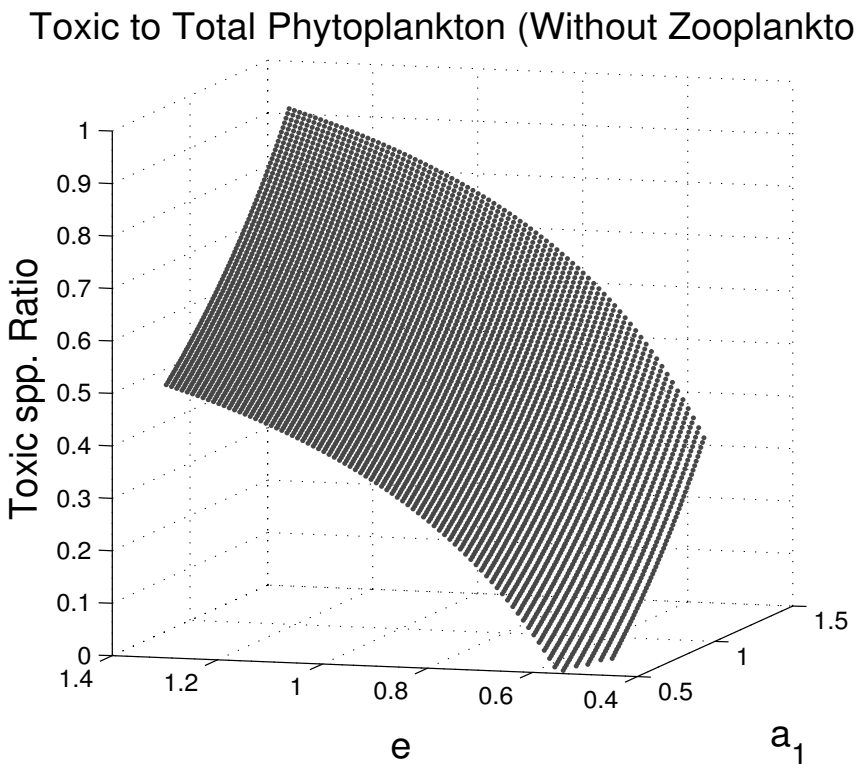

Figure 13: Comparison of the effect of toxic spp. nitrogen uptake rate (a_1) vs. their predation on the non-toxic spp. (e) and their effects on the ratio $\frac{T}{N+T}$. In this case we do not consider the effect from the zooplankton population and we see that the ratio $\frac{T}{N+T}$ is much higher than when zooplankton are considered.

This research was undertaken with the goal of finding out how we could reduce the ratio of toxic spp. population in the total population of phytoplankton. With this end in mind we analyzed our model, and studied how the parameters affect the ratio of interest. For this section, we will consider the effect of parameters a_1 (nitrogen uptake by the toxic *Protoperidinium* spp.) and e (predation of toxic on non-toxic). Only coexistence equilibria are considered when studying how these parameters affect the population ratio. Figures 12 and 13 only show points in which all populations exist. By analyzing our graphs we can see that for the case in which zooplankton is not considered, the ratio of toxic population to total phytoplankton population is much higher than when zooplankton is considered. This is due to a higher predation rate on toxic phytoplankton by zooplankton. Therefore, the toxic phytoplankton population is more strongly affected by the higher predator.

7 Uncertainty Analysis

To fully inspect the ratio of *Protoperidinium* to total phytoplankton $\left(\frac{T}{N+T}\right)$ as we have set out to do, uncertainty analysis is utilized to determine which of our parameters has the greatest effect on this ratio. The greater the effect means the estimated values for these parameters are very important, and should be calculated with as much accuracy as possible as they could alter results dramatically.

We use the method of Latin Hypercube Sampling (LHS) to determine the effect our parameters have on the ratio of *Protoperidinium* to total phytoplankton. LHS is a method that is especially useful for our purposes, as we have a high amount of parameters. Compared to pure random sampling, the method of LHS requires fewer sampling runs and still produces the same accuracy. LHS is conducted by separating the parameter range into n sections, each with the same probability of being chosen from. This is done to guarantee that the entire sampling area is explored. Samplings for each variable are taken. They then produce output for the ratio by randomly mixing samplings for each parameter value . The samplings as well as the output are then rank transformed to fit the linear model [14]. From this, the partial rank correlation coefficient (PRCC) is calculated between $(-1, 1)$ and used to produce Figure 14.

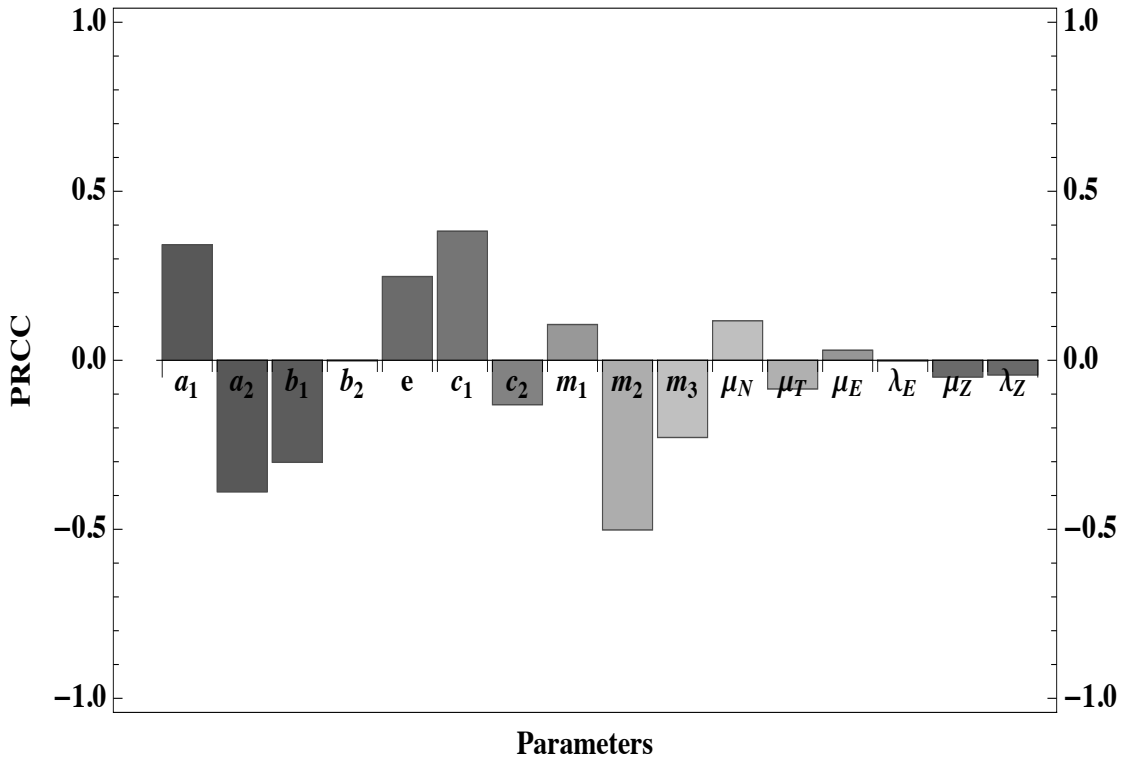

Figure 14: Uncertainty analysis of the ratio $\frac{T}{N+T}$ and the parameters of our system.

From our analysis and the given results in Figure 14 we see that the parameters a_1, a_2, b_1,

e, c_1, c_2, m_1, m_2, m_3, and μ_N have the greatest effect on the ratio $\frac{T}{N+T}$. Recall these particular parameters are dependent on the species we choose to model using our equations. Although the ratio is not affected as significantly by λ_E as compared to the parameters listed above, we demonstrated in Section 6 that variation of this parameter still affects the ratio enough to meet our purposes.

We now examine the meaning of Figure 14 in detail to understand how our parameters affect the model and ratio of toxic to total phytoplankton. Notice in the figure that a_1, e, c_1, m_1, and μ_N are of the same sign, and that the sign is opposite of a_2, b_1, c_2, m_2, and m_3. Notice that the meaning of the parameters with positive PRCC are consumption of nutrients by toxic phytoplankton, predation on non-toxic by toxic phytoplankton, mass conversion from nutrients to toxic phytoplankton, mass conversion from non-toxic to toxic phytoplankton, and outflow of non-toxic phytoplankton. It is no surprise that increasing these parameters would also increase the ratio of toxic to total phytoplankton. This corresponds to the fact that the parameters with positive PRCC increase the ratio.

Recall that the remaining parameters of significance, a_2, b_1, c_2, m_2, and m_3 represent consumption of nutrients by non-toxic phytoplankton, predation by the zooplankton on toxic phytoplankton, mass conversion from nutrients to non-toxic phytoplankton, mass conversion of toxic phytoplankton to zooplankton, and mass conversion from non-toxic to zooplankton, respectively. It is intuitive that an increase in each of these parameters will simultaneously decrease the ratio as they will either decrease the number of toxic phytoplankton in the system or increase the number of non-toxic phytoplankton.

Our analysis suggests that our model could be used to show relationships between other species, but exploring different species is beyond the scope of this project. It appears that this type of sensitivity analysis would be most helpful in deciding either what direction to go in or what species to look into as future research. Thus, we conclude that in order to reduce the ratio for the species we chose and their associated parameter values, we should look at the remaining parameters that we can alter, such as λ_E. This would allow us to better guess the interactions between different species.

8 Discussion

Our goal was to study how to lower the ratio of toxic phytoplankton to total phytoplankton in a coexisting environment. We found that mutual predation by a zooplankton spp., such as *Chaetognaths*, has a greater detrimental effect on the toxic spp. *Protoperidinium* than on the non-toxic spp. We attributed the fact that *Chaetognaths* reduces our ratio of interest to the fact that it senses its prey by vibration. Since *Protoperidinium* is bigger than *Heterocapsa* it is easier to find and predate upon. Therefore, we infer that the predation rate on *Protoperidinium* would be much higher relative to that of *Heterocapsa*.

We also found that one of the most important parameters of our system was how efficient the two phytoplankton types were at obtaining nitrogen from the environment. By varying the turnover rate of nitrogen ($\frac{\lambda_E}{\mu_E}$), we could control the ratio of toxic to total phytoplankton in a coexisting environment. For practical purposes, controlling the turnover rate is much more useful and feasible than altering nitrogen consumption rates that vary mainly by species. For further work, studies could include more in-depth work where nitrogen uptake and nitrogen turnover rate are concerned,

as these are critical when considering the ratio. Our model would also be useful in examining other species and environments to monitor effects on the ecosystem, human health, and economy.

Acknowledgments

We would like to thank Dr. Carlos Castillo-Chavez, Executive Director of the Mathematical and Theoretical Biology Institute (MTBI), for giving us the opportunity to participate in this research program. We would also like to thank Co-Executive Summer Directors Dr. Erika T. Camacho and Dr. Stephen A. Wirkus for their efforts in planning and executing the day to day activities of MTBI. We thank Kamal Barley for providing help in redrawing the figures. This research was conducted in MTBI at the Mathematical, Computational and Modeling Sciences Center (MCMSC) at Arizona State University (ASU). This project has been partially supported by grants from the National Science Foundation (NSF - Grant DMPS-1263374), the National Security Agency (NSA - Grant H98230-13-1-0261), the Office of the President of ASU, and the Office of the Provost of ASU.

References

[1] J Adams. The definition and interpretation of guild structure in ecological communities. *The Journal of Animal Ecology*, pages 43–59, 1985.

[2] Priyanga Amarasekare. Coexistence of intraguild predators and prey in resource-rich environments. *Ecology*, 89(10):2786–2797, 2008.

[3] Robert D Barnes and Edward E Ruppert. *Invertebrate zoology*. WB Saunders Philadelphia, 1968.

[4] Douglas G Capone, Deborah A Bronk, Margaret R Mulholland, and Edward J Carpenter. *Nitrogen in the marine environment*. Access Online via Elsevier, 2008.

[5] Zoe V Finkel, John Beardall, Kevin J Flynn, Antonietta Quigg, T Alwyn V Rees, and John A Raven. Phytoplankton in a changing world: cell size and elemental stoichiometry. *Journal of Plankton Research*, 32(1):119–137, 2010.

[6] Deborah R Hart. Intraguild predation, invertebrate predators, and trophic cascades in lake food webs. *Journal of Theoretical Biology*, 218(1):111–128, 2002.

[7] Robert D Holt and Gary A Polis. A theoretical framework for intraguild predation. *American Naturalist*, pages 745–764, 1997.

[8] Carlton D Hunt, David G Borkman, P Scott Libby, Richard Lacouture, Jefferson T Turner, and Michael J Mickelson. Phytoplankton patterns in massachusetts bay—1992–2007. *Estuaries and coasts*, 33(2):448–470, 2010.

[9] Kevin J James, Cian Moroney, Cilian Roden, Masayuki Satake, Takeshi Yasumoto, Mary Lehane, and Ambrose Furey. Ubiquitous 'benign'alga emerges as the cause of shellfish contamination responsible for the human toxic syndrome, azaspiracid poisoning. *Toxicon*, 41(2):145–151, 2003.

[10] HJ Jeong and Michael I Latz. Growth and grazing rates of the heterotrophic dinoflagellates protoperidinium spp. on red tide dinoflagellates. *Marine Ecology-Progress Series*, 106:173–173, 1994.

[11] Uwe John, Urban Tillmann, and Linda K Medlin. A comparative approach to study inhibition of grazing and lipid composition of a toxic and non-toxic clone of chrysochromulina polylepis (prymnesiophyceae). *Harmful Algae*, 1(1):45 – 57, 2002.

[12] MI Latz and HJ Jeong. Effect of red tide dinoflagellate diet and cannibalism on the bioluminescence of the heterotrophic dinoflagellates protoperidinium spp. *Marine ecology progress series. Oldendorf*, 132(1):275–285, 1996.

[13] Margaret-Rose Leung, Dustin Padilla, Noah Shemer, Juan Vinagera, and Baojun Song. A symmetric intraguild predation model for the invasive lionfish and native grouper. 2011.

[14] Simeone Marino, Ian B. Hogue, Christian J. Ray, and Denise E. Kirschner. A methodology for performing global uncertainty and sensitivity analysis in systems biology. *Journal of Theoretical Biology*, 254(1):178 – 196, 2008.

[15] Susanne Menden-Deuer, Evelyn J Lessard, Jessi Satterberg, and Daniel Grünbaum. Growth rates and starvation survival of three species of the pallium-feeding, thecate dinoflagellate genus protoperidinium. *Aquatic microbial ecology*, 41(2):145–152, 2005.

[16] Shane O'Boyle and Joe Silke. A review of phytoplankton ecology in estuarine and coastal waters around ireland. *Journal of plankton research*, 32(1):99–118, 2010.

[17] Irina Olenina. Biovolumes and size-classes of phytoplankton in the baltic sea. *Baltic Sea Environment Proceedings No.106*, 2006.

[18] Morten Foldager Pedersen and Jens Borum. Nutrient control of algal growth in estuarine waters. nutrient limitation and the importance of nitrogen requirements and nitrogen storage among phytoplankton and species of macroalgae. *Marine ecology progress series. Oldendorf*, 142(1):261–272, 1996.

[19] Gary A Polis, Christopher A Myers, and Robert D Holt. The ecology and evolution of intraguild predation: potential competitors that eat each other. *Annual review of ecology and systematics*, 20:297–330, 1989.

[20] Alan J Southward, Olivia Langmead, Nicholas J Hardman-Mountford, James Aiken, Gerald T Boalch, Paul R Dando, Martin J Genner, Ian Joint, Michael A Kendall, Nicholas C Halliday, et al. Long-term oceanographic and ecological research in the western english channel. *Advances in Marine Biology*, 47:1–105, 2004.

[21] Michael J Twiner, Nils Rehmann, Philipp Hess, and Gregory J Doucette. Azaspiracid shellfish poisoning: a review on the chemistry, ecology, and toxicology with an emphasis on human health impacts. *Marine drugs*, 6(2):39–72, 2008.

[22] Peter G Verity, Charles Y Robertson, Craig R Tronzo, Melinda G Andrews, James R Nelson, and Michael E Sieracki. Relationships between cell volume and the carbon and nitrogen content of marine photosynthetic nanoplankton. *Limnology and Oceanography*, 37(7):1434–1446, 1992.

[23] Mineo Yamaguchi, Shigeru Itakura, and Takuji Uchida. Nutrition and growth kinetics in nitrogen-or phosphorus-limited cultures of the'novel red tide'dinoflagellate heterocapsa circularisquama (dinophyceae). *Phycologia*, 40(3):313–318, 2001.

Appendix A

Proof of Theorem 2 We compute the Jacobian matrix of the system of equations (5)-(8) in order to analyze the stability of the NTPFE equilibria.

$$\begin{bmatrix} -N_3^* a_2 - T_3^* a_1 - \mu_E & -a_2\, E_3^* & -a_1\, E_3^* & 0 \\ N_3^* a_2\, c_2 & F_1 & -N_3^* e & -N_3^* b_2 \\ T_3^* a_1\, c_1 & m_1\, eT_3^* & F_2 & -T_3^* b_1 \\ 0 & Z_3^* b_2\, m_3 & Z_3^* b_1\, m_2 & F_3 \end{bmatrix}$$

Where:

$$\begin{aligned} F_1 &= a_2\, E_3^* c_2 - T_3^* e - Z_3^* b_2 - \mu_N \\ F_2 &= a_1\, E_3^* c_1 + N_3^* e m_1 - Z_3^* b_1 - \mu_T \\ F_3 &= N_3^* b_2\, m_3 + b_1\, m_2\, T_3^* - \mu_Z \end{aligned}$$

Next we evaluate this Jacobian matrix at our equilibrium point of $(E_3^*, N_3^* = 0, T_3^*, Z_3^*)$

$$\begin{bmatrix} -T_3^* a_1 - \mu_E & -a_2\, E_3^* & -a_1\, E_3^* & 0 \\ 0 & a_2\, E_3^* c_2 - T_3^* e - Z_3^* b_2 - \mu_N & 0 & 0 \\ T_3^* a_1\, c_1 & m_1\, eT_3^* & a_1\, E_3^* c_1 + -Z_3^* b_1 - \mu_T & -T_3^* b_1 \\ 0 & Z_3^* b_2\, m_3 & Z_3^* b_1\, m_2 & b_1\, m_2\, T_3^* - \mu_Z \end{bmatrix}$$

We can see that the item in the second row, second column position is the only nonzero element in the second row. Therefore $a_2 E_3^* c_2 - T_3^* e - Z_3^* b_2 - \mu_N$ is an eigenvalue and must be less than zero in order to have a stable system. So we have one condition for stability at the $NTPFE$ equilibrium is

$$a_2 E_3^* c_2 < T_3^* e + Z_3^* b_2 + \mu_N$$

In our 4 by 4 Jacobian, we can eliminate the second row and second column and reduce the Jacobian to a 3 by 3 matrix. Also note that if we factor T out of equation (7), we have

$$(a_1 c_1 E_3^* - b_1 Z_3^* - \mu_T) T_3^* = 0.$$

Since T cannot be zero for the NTPFE case, $a_1c_1E_3^* - b_1Z_3^* - \mu_T$ must be zero in order to insure stability. So our reduced Jacobian is

$$\begin{bmatrix} -T_3^*a_1 - \mu_E & -a_1\,E_3^* & 0 \\ T_3^*a_1\,c_1 & 0 & -T_3^*b_1 \\ 0 & Z_3^*b_1\,m_2 & b_1\,m_2\,T_3^* - \mu_Z \end{bmatrix}$$

To analyze the stability of this equilibrium point, we apply Routh-Hurwitz criterion to the 3 by 3 matrix.

$$W_1 = -(det|Jacobian|) = -[(-a_1T_3^* - \mu_E)[(b_1m_2T_3^*b_1Z_3^*)] - (-a_1E_3^*)(a_1c_1T_3^*)(b_1m_2T_3^* - \mu_Z)]$$

One requirement for stability is $W_1 > 0$, which is

$$(a_1T_3^* + \mu_E)(b_1m_2T_3^*b_1Z_3^*) + (a_1E_3^*)(a_1c_1T_3^*)(\mu_Z - b_1m_2T_3^*) > 0$$

We see that if $\mu_Z - b_1m_2T_3^* > 0$, then $W_1 > 0$. Therefore

$$\frac{\mu_Z}{b_1m_2} > T_3^* \quad \text{or} \quad \frac{\mu_Z}{b_1m_2} > \frac{-B \pm \sqrt{B^2 - 4AC}}{2A}$$

Now we compute $W_2 = -Tr(Jacobian) = a_1T_3^* + \mu_E + (\mu_Z - b_1m_2T_3^*) > 0$. If we assume $\mu_Z - b_1m_2T_3^* > 0$ as in the case for $W_1 > 0$, then we have $W_2 > 0$, and our second Routh-Hurwitz criterion is met.

Next we compute W_3, our third Routh-Hurwitz criterion, which dictates we must have $W_3 > 0$ $W_3 > 0$ is equivalent to $(a_1E_3^*)(a_1c_1T_3^*) + (b_1T_3^*)(b_1m_2Z_3^*) + (-a_1T_3^* - \mu_E)(b_1m_2T_3^* - \mu_Z) > 0$. This is

$$(a_1E_3^*)(a_1c_1T_3^*) + (b_1T_3^*)(b_1m_2Z_3^*) + (a_1T_3^* + \mu_E)(\mu_Z - b_1m_2T_3^*) > 0$$

Again, if $\mu_Z - b_1m_2T_3^* > 0$, then $W_3 > 0$.

Finally, we check $W_2W_3 > W_1$.

$$W_2W_3 = (a_1T_3^* + \mu_E)(b_1T_3^*)(b_1m_2Z_3^*) + (\mu_Z - b_1m_2T_3^*)(a_1E_3^*)(a_1c_1T_3^*) +$$
$$(a_1T_3^* + \mu_E[a1E_3^*)(a_1c_1T_3^*) + (a_1T_3^* + \mu_E)(\mu_Z - b_1m_2T_3^*)] +$$
$$(\mu_Z - b_1m_2T_3^*)[(b_1T_3^*b_1m_2Z_3^*) + (a_1T_3^* + \mu_Z - b_1m_2T_3^*)]$$

Once again we assume $\mu_Z - b_1m_2T_3^* > 0$. Note that $W_2W_3 = W_1 + X$ where $X =$

$$(a_1T_3^* + \mu_E[a1E_3^*)(a_1c_1T_3^*) + (a_1T_3^* + \mu_E)(\mu_Z - b_1m_2T_3^*)] +$$
$$(\mu_Z - b_1m_2T_3^*)[(b_1T_3^*b_1m_2Z_3^*) + (a_1T_3^* + \mu_Z - b_1m_2T_3^*)]$$

$W_2W_3 = W_1 + X$ implies that $W_2W_3 > W_1$. Therefore, we can conclude that if both condition (1) (Eigenvalue $\lambda_1 < 0$) and condition (2) $\mu_Z - b_1m_2T_3^* > 0$ are met, then we will have a stable (NTPFE) boundary equilibria.

Appendix B

Special Cases From Section 4.4
We now explore the special cases

$$\begin{aligned} b_2 m_3 F - b_1 m_2 B &= 0 \\ A_1 &= 0 \end{aligned}$$

from the PCE. These cases were chosen because they can be used to reduce the quartic equation of N to a cubic equation.

Case 1: $b_2 m_3 F - b_1 m_2 B = 0$
We now make the proper substitutions into our first case and arrive at:

$$b_2 m_3 \left(\frac{b_1}{m_1 e}\right) - b_1 m_2 \left(\frac{b_2}{e}\right) = 0$$

Reducing, we attain:

$$m_1 m_2 = m_3$$

which is equivalent to both

$$m_1 = \frac{m_3}{m_2} \qquad\qquad m_2 = \frac{m_3}{m_1}$$

Examining this conclusion biologically yields interesting, but unrealistic results. It states that the loss of nutrients when a zooplankton eats a non-toxic phytoplankton is greater than the loss from non-toxic to toxic and toxic to zooplankton. Trophic efficiency is a clear counterargument to this statement. Still, assuming this condition is true, we achieve the cubic equation:

$$U_1 E^3 + U_2 E^2 + U_3 E + U_4$$

where

$$\begin{aligned} U_1 &= A_1 b_1 m_2 A - A_1 b_2 m_3 D \\ U_2 &= A_1 b_2 m_3 G - A_1 b_1 m_2 C - A_1 \mu_z + A_2 b_1 m_2 A - A_2 b_2 m_3 D \\ U_3 &= \lambda_Z - A_3 b_1 m_2 A + A_3 b_2 m_3 D - b_1 m_2 A_2 C + A_2 b_2 m_3 G - A_2 \mu_z \\ U_4 &= A_3 b_1 m_2 c - A_3 b_2 m_3 G + A_3 \mu_z \end{aligned}$$

Case 2: $A_1 = 0$

Looking specifically at the term A_1, we see that this is equivalent to:

$$\frac{a_1 a_2 c_2}{e} - \frac{a_1 a_2 c_1}{m_1 e} = 0$$

Simplification yields:

$$m_1 = \frac{c_1}{c_2}$$

Biologically this case means that all nitrogen is retained when a toxic phytoplankton consumes a non-toxic one. Again, this condition is unlikely. Similar to the first condition, we are left with a cubic equation:

$$V_1 E^3 + V_2 E^2 + V_3 E + V_4$$

where

$$\begin{aligned}
V_1 &= b_1 m_2 A A_2 - b_2 m_3 D A_2 \\
V_2 &= \lambda_z - b_1 m_2 A A_3 + b_2 m_3 D A_3 - b_1 m_2 B (A_2)^2 - b_1 m_2 C A_2 + b_2 m_3 F (A_2)^2 + b_2 m_3 G A_2 - \mu_z A_2 \\
V_3 &= b_1 m_2 B A_2 A_3 + b_1 m_2 C A_3 - b_2 m_3 F A_2 A_3 - b_2 m_3 G A_3 + \mu_z A_3 + b_1 m_2 B A_3 A_2 - b_2 m_3 A_3 F A_2 \\
V_4 &= b_1 m_2 B (A_3)^2 - b_2 m_3 F (A_3)^2
\end{aligned}$$